A Satisficing Conflict Resolution Approach for Multiple UAVs

Yumeng Li, *Student Member, IEEE*, Wenbo Du, *Member, IEEE*, Peng Yang, Tianhang Wu, Jun Zhang, Dapeng Wu, *Fellow, IEEE*, and Matjaž Perc

***Abstract*—In this paper, we are concerned with exploring the theoretically and technically research outcomes for the conflict resolution (CR) of multiple unmanned aerial vehicles (UAVs) by using the Internet of Things technologies. We propose a satisficing algorithm to mitigate the CR problem of multiple UAVs. Specifically, we first formulate the CR problem as a game model and design strategies of the game model based on flight characteristics of UAVs. Next, a satisficing game theory is used to mitigate the formulated problem. Furthermore, required time of arrival, which is a new judgment parameter of the strategy utility, is developed to ensure that the whole system can reach a socially acceptable compromise. Simulation results verify the effectiveness and adaptability of the proposed algorithm under complex environments.**

***Index Terms*—Conflict resolution (CR), cooperative control, satisficing game theory.**

I. Introduction

TODAY, unmanned aerial vehicles (UAVs) are finding increasingly wide utilization in civil aviation and military affairs [1]. Generally, UAVs are controlled and operated by a centralized ground station, and the operation range is always limited to urban areas [2]. The Next-Generation Air Transportation System has proposed a free-flight concept [3], [4], allowing flights (manned and unmanned) to change their routes without approval from the centralized management unit. Therefore, navigable aircraft typically employ a free-flight mode in which the aircraft does not have to travel along the routes and routes of a series of navigation platforms. But according to the current situation, custom flight along the fastest and most economical route. To this aim, decentralized control schemes are urgently required. It is, however, high challenging to realize the decentralized control of airborne platforms. Internet of Things (IoT) technologies presents unique advantages in solving this problem [5]–[7]. In IoT technologies, a UAV can act as a mobile aerial [8], [9], which can sense the surrounding and provide on-the-fly communications with many other UAVs about their information, to perform conflict avoidance maneuver autonomously.

Furthermore, the latest investigation by the federal aviation administration indicates that there may be 7 million UAVs flying in the United States in 2020 [10]. Due to the complex environment of low-altitude airspace, the security of low-altitude aircraft is greatly threatened by the constraints of complex environment given various landform, extreme weather conditions and air vehicles of all kinds. Thus, the traditional centralized governance method is not suitable for this conflict avoidance problem. Therefore, requiring decentralized algorithms to avoid collisions and obstacles may be one crucial issue [11]. Conflict resolution (CR), aiming at providing effective solutions to eliminate potential vehicle conflicts, is an important technique to ensure such a safe vehicle operation.

In the last decade, a large number of CR approaches have been proposed, most of which being mainly focused on geometric approaches. Geometric approaches utilize the geometric characteristics of aircraft trajectories to avoid vehicles' conflict [12]. It uses polynomials to express the solution of CR. Therefore, it is generalized, high efficient and simple to calculate. Chakravarthy and Ghose [13] introduced a conflict detection and avoidance method in a 2-D dynamic environment based on nuclear collision theory. It lays the foundation for geometrics approaches to aircraft CR. Bilimoria [14] proposed a method that can deduce the geometrical shape of a conflict scene within a certain time in the future according to the location, velocity, and heading of the aircraft. Mao *et al.* [15] proved the closed-loop stability of two intersecting flows of aircraft under decentralized sequential CR schemes. Tang *et al.* [16] presented an improved geometric optimization algorithm for cooperative UAVs sharing a 3-D airspace. This method aims to provide a feasible optimal trajectory for the selected UAV with a local optimization scope

Manuscript received April 29, 2018; revised October 30, 2018; accepted November 27, 2018. Date of publication December 5, 2018; date of current version May 8, 2019. This work was supported in part by the National Key Research and Development Program of China under Grant 2016YFB1200100, in part by the National Natural Science Foundation of China under Grant 61425014, Grant 61521091, Grant 91538204, Grant 61671031, Grant 61722102, and Grant 91738301, and in part by the Slovenian Research Agency under Grant J1-7009 and Grant P5-0027. *(Corresponding authors: Wenbo Du; Jun Zhang.)*

Y. Li is with the School of Electronic and Information Engineering, Beihang University, Beijing 100191, China, with the Key Laboratory of Advanced Technology of Near Space Information System (Beihang University), Ministry of Industry and Information Technology of China, Beijing 100191, China, and also with Shen Yuan Honors College, Beijing 100191, China.

W. Du, P. Yang, and T. Wu are with the School of Electronic and Information Engineering, Beihang University, Beijing 100191, China, and also with the Key Laboratory of Advanced Technology of Near Space Information System (Beihang University), Ministry of Industry and Information Technology of China, Beijing 100191, China (e-mail: wenbodu@buaa.edu.cn).

J. Zhang is with the School of Information and Electronics, Beijing Institute of Technology, Beijing 10081, China (e-mail: buaazhangjun@vip.sina.com).

D. Wu is with the Department of Electrical and Computer Engineering, University of Florida, Gainesville, FL 32611 USA.

M. Perc is with the Faculty of Natural Sciences and Mathematics, University of Maribor, 2000 Maribor, Slovenia, and also with the Center for Applied Mathematics and Theoretical Physics, University of Maribor, 2000 Maribor, Slovenia.

Digital Object Identifier 10.1109/JIOT.2018.2885147

at the operational level. Although most of these approaches can obtain good performance, they cannot guarantee optimal solutions under a multiagents scenario.

In past decades, the potential field approach [17] found widespread use as a navigation method for ground robots and more recently for UAVs. For example, Eby [18] introduced the potential field method to solve the aircraft conflict problem. They planned the path of aircraft by the attraction and repulsion in a potential and vortex field. Xiang *et al.* [19] proposed an artificial potential field model that combined turning and evaluation constraints and calculated the influencing radii of obstacles. For more information, the reader can refer to [20] and [21] and the references therein. Although the potential field approach can solve the conflicts of vehicles effectively, it has some inherent limitations. This method cannot easily find paths through narrow passages. Additionally, since the potential function requires to be designed heuristically for every problem, it will be computationally heavy to see them within obstacle-laden spaces. What is more, the potential field method will obtain some impractical solutions when turning angles of vehicles are limited.

Game theory, as a mathematical model for solving conflicts of interest and optimizing resource allocation, has received extensive attention in recent decades, which has been deeply applied in economic policy [22], resource allocation in wireless networks [23]–[26], and task scheduling [27]. The basic assumption is that the parties in the game refer to their respective knowledge and the intention of the other party to perform corresponding operations according to their own goals. In recent years, the application research of game theory in the field of air traffic is gradually emerging and has received encouraging initial results. Pappas *et al.* [28] proposed a decentralized conflict architecture that views the aircraft as a hybrid system incorporating both discrete events and individual dynamics modeled by differential equations. For CR, noncooperative methods from game theory are used by each aircraft to search for a velocity change that guarantees separation regardless of the actions of the opponent. The noncooperative game-theoretic approach is expanded in [29] to include both path deviations and speed variations. Several approaches formulate CR as a game [30]–[33]. In their models, individuals are divided into evaders and pursuers. An evader tries to avoid a collision against all possible pursuer's maneuvers. Such game-theoretic approach is very useful for noncooperative cases, where aircraft cannot communicate together, and it also has the advantage of the low time complexity in practice.

In recent years, Archibald *et al.* [34] presented a decentralized and multiagent approach based on satisficing game theory to resolve conflicts in the en-route airspace. Without centralized control or global knowledge, this approach varies from the perspective of each participant. Satisficing permits group and individual interests to be reconciled in a single, coherent mathematical structure. They introduced a new concept-social utility that represents the influences on the remaining aircraft from the current strategy. Aircraft avoid conflicts by choosing a strategy according to this utility parameter. This approach, however, does not consider the following problems.

1) Uncertainty factors have not been addressed in conflict detection.
2) During the process of CR, this CR approach avoids conflicts only through heading-change (HC) maneuvers. In an air traffic control system, the velocity of a vehicle plays a crucial role in CR.
3) This proposed method does not consider the complexity environments, e.g., static deterrents.

In this paper, we propose a decentralized CR approach that guarantees the safety of a UAV when flying in an environment with the obstacle. It shows that our approach can resolve the conflict of multiple aircrafts efficiently and is also robust to complex situations. The contributions of this paper can be summarized as the following.

1) We formulate a CR problem into a game theory one. The game neighbors of an aircraft are the aircrafts within its detection range. Besides, we present a priority ranking mechanism to ensure the success of the updating strategy.
2) We design mixed strategies of changing both the heading and the velocity in the game model. These strategies are related to UAV flight characteristics. Herein, a parameter, required time of arrival (RTA), is developed to evaluate utilities of strategy by comparing actual flight time with the RTA.
3) We introduce accessibility scenes and obstacle scenes to implement our approach, which establishes a complex environment.

The remainder of this paper is as follows. The next section describes the system model for this paper. Section III describes the CR algorithm constructed within the satisficing framework. Section IV describes the simulator used and presents simulation results from a variety of conflict scenarios. Section V summarizes our findings and concludes this paper.

II. System Model

The prevailing conflict avoidance process is composed of two aspects: 1) conflict detection and 2) CR. The conflict detection problem concerns detecting potential conflicts on the aircraft trajectories and searching for a CR; the CR problem concerns finding a set of appropriate strategies for each aircraft involved in conflicts that are individual-interest-satisfied while also being conflict-free globally.

UAV communication plays an essential role in conflict detection [35]–[37]. We assume that the UAV can collect information of all other aircraft, obstacles or threats within a 10 nmi radius (R_d) using IoT technologies. Each aircraft is equipped with the global positioning system (GPS) and automatic dependence surveillance-broadcast that broadcasts information about its location and intentions to all other aircraft within the radius R_d. This information includes current position, destination, heading angle, velocity, flight time, and delay (relative to an unobstructed straight-line flight). There are two different types of separate violations for aircrafts that must be noticed, i.e., collisions, when an aircraft comes within 500 ft (R_c) of another, and near misses, when aircraft are separated by less than 1 nmi (R_{nm}) (as depicted in Fig. 1).

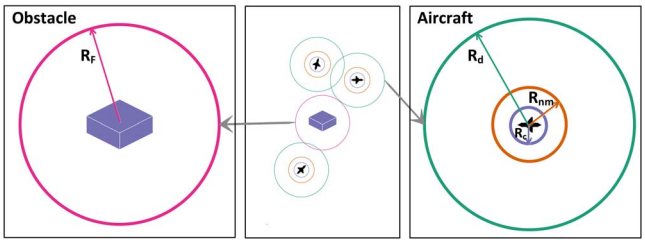

Fig. 1. Forbidden zone for an obstacle. Near miss and collision zone for an aircraft.

For those deterrents, we only have their location information. Thus, we just define a forbidden zone (R_F) around the deterrent, as shown in Fig. 1. UAVs are not allowed to fly over this zone to keep a safe distance to threats.

A. Conflict Detection

For conflict detection, each UAV ensures the potential game neighbors over IoT technology first. Then, we applied the closest-point-of-approach (CPA) method to predict the future position of the potential game neighbors in order to judge the actual game neighbors. Herein, we also consider that the GPS system is influenced by wind or other complex environments, which result in position uncertainty. In this section, we explain the conflict detection process in detail.

1) IoT Technology: IoT technology is applied in the identification of UAVs' potential neighbors which are within their detection range. The specific implementation process is as follows.

1) UAV A periodic broadcast "hello packets" within the detection range. The maximum range of signal transmission is defined as the detection range.
2) Individuals within the detection range of UAV A will receive the packets. For example, after UAV B received the hello packets, it need to reply an ACK message to the target UAV. The ACK message include current velocity, position and heading, destination, flight time, and delay (relative to an unobstructed straight-line flight).
3) UAV A can know its neighbor UAVs and obtain the needed information through eavesdropping and parsing ACK packets.

2) Closest Point of Approach: In our method, we use the deterministic-type CPA method [38] for conflict detection. We can extrapolate the UAV's future condition from the current state. Let U represent the set of all aircraft within a given en-route airspace area, where each aircraft $u_i (u_i \in U)$ is surrounded by two virtual cylinders: 1) the near miss and 2) collision zone. As shown in Fig. 2, T_w represents the predicted time; we forecast the flight path of u_i and u_j ($u_i, u_j \in U$; $i, j = 1, \ldots, n$ and $i \neq j$) utilizing their current state vectors in the next T_w time and then calculate the minimum distance $d_{\min}(i, j)$ between these two UAVs within this period. We define $d_{k\min}(i, j)$ as the distance between the starting point and the location of the aircraft arriving at $d_{\min}(i, j)$. The current position of u_c^i is $(x_c^i,\ y_c^i)$, heading angle is Ang_c^i,velocity is v_c^i; the predicted position u_t^i can be described as follows:

$$u_t^i = \left\{\left(x_t^i, y_t^i\right)\right\}_{t=1}^{T_w}$$

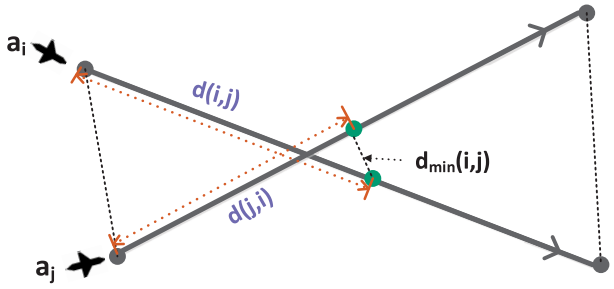

Fig. 2. Conflict prediction schematic diagram.

$$\begin{aligned} x_t^i &= v_c^i \cdot t \cdot \cos\left(\mathrm{Ang}_c^i\right) \\ y_t^i &= v_c^i \cdot t \cdot \sin\left(\mathrm{Ang}_c^i\right). \end{aligned} \tag{1}$$

A conflict or loss of separation between two aircraft x_i and x_j occurs within this area whenever the near miss or collision zones of the aircraft overlap. We use R_c and $R_{\mathrm{nm}} (R_c < R_{\mathrm{nm}})$ to denote the collision radius and near miss radius, respectively. Therefore, a collision event occurs if $d(i, j) \leq R_c$, and a near miss event occurs if $d_{\min}(i, j) < R_{\mathrm{nm}}$; here, $d(i, j)$ refers to the distance between x_i and x_j. $E_c(i, j)$ and $E_{\mathrm{nm}}(i, k)$ denote collision and near miss event, respectively, and $E_i = \bigcup_{jk}(E_c(i, j) \cup E_{\mathrm{nm}}(i, k))$ is all the conflict events concerning aircraft. In addition, we call E_i the conflict space. Thus, We represent a conflict event between two aircraft as $E_{ij} = (d(i, j), d_{\min}(i, j))$.

During the predicted period T_ws, there may be more than one conflict risk or collision of x_i. Therefore, the set of conflict events defined as

$$E_i = \left\{E_{ij} | i = 1, \ldots, i-1, i+1, \ldots, N\right\}. \tag{2}$$

In this way, the CR problem can be described as the game between x_i and its potential conflict set E_i.

3) Position Uncertainty Model: Uncertainty can be modeled using (approximated) probabilistic methods [39]–[41]. In this paper, we only consider that the GPS system is influenced by wind or other complex environments, which result in position uncertainty. In the civil field, GPS systems have a horizontal accuracy of five to ten meters with ninety-five percent confidence, and the vertical accuracy is approximately 1.4 times the horizontal accuracy [42]. Therefore, small errors of the GPS may accrue large position uncertainties.

In this section, a simple bivariate Gaussian model is utilized for the uncertainties. Given independent and isotropic GPS horizontal accuracies, the UAV position density function p can be expressed as

$$p\left(x_i, y_i, \sigma_x, \sigma_y\right) = \frac{1}{2\pi\sigma_x\sigma_y} e^{-\left(\frac{(x-x_i)^2}{2\sigma_x^2} + \frac{(y-y_i)^2}{2\sigma_y^2}\right)} \tag{3}$$

where σ_x and σ_y are the standard deviations and $\vec{s}_i = (x_i, y_i)$ is the coordinate of the center point of the position uncertainty model.

Given a normal distribution $X \sim (\mu, \sigma^2)$, we have the famous 3σ principle, $P(\mu - 3\sigma < X \leq \mu + 3\sigma) = 99.7\%$, i.e.,

if an event $X \notin (\mu - 3\sigma, \mu + 3\sigma]$, then its occurrence probability is almost zero. Similarly, we apply this 3σ principle in this paper to restrict the above-mentioned probability circle.

B. Conflict Resolution Model Formulation

The essence of the CR problem is to find a feasible set of maneuvering strategies for all individual aircraft involved in the conflict to ensure the safety of the flights. The evolutionary game is a very natural analysis involving potential conflicts of interest. The game must be played through interactive negotiation between individuals to reach the theoretical framework of the group goal problem. Therefore, we propose a decentralized CR method based on game theory. This method not only solves the flight conflict problem at the group level but also maximizes the benefits of each aircraft at the individual level.

1) Conflict Game Model: We assume the CR problem as a cooperative multiagent game model, in which each has a set of feasible candidate policies. In our model, the aircraft can communicate with each other to obtain flight information of other aircraft within the detection range over IoT technology [43]. During the forecast period, E_i are a set of aircraft x_i involved in all potential conflicts. In our CR method, the release of E_i can be regarded as an n-person cooperative game. Game players are UAVs ($x_i, i = 1, 2, \ldots, N$) from the candidate strategy set S_i,$s_i^n \in S_i$. $P(s_i^n)$ denotes the game payoff, which is calculated using the strategy set ($s_1^n, s_2^n, s_i^n, s_M^n$) between x_i and its neighboring aircraft. The conflict prediction function stated in the previous section can be mathematically constructed as $H : S_i \times S_j \rightarrow W^2$, which maps the two players' strategy space to the CR strategy space.

2) Game Neighbor Selection: Using the conflict detection information, the game neighbors of an aircraft are the aircraft within its detection range and that have a risk of potential collision. Thus, how to produce a valid priority ranking of all aircraft is the essential task.

Herein, we formulate a priority ranking mechanism to ensure the asynchronous strategy updating order. In our model, a player with a higher ranking will only satisfy its interests entirely when making a decision; a player with a lower ranking is more conflict sensitive and can change its own optimal choices to benefit the group. Generally, the ranking is established by an environmental risk assessment, the flight delay, the remaining fuel endurance and the proximity to the destination. The rules of status allocation are as follows.

1) For all aircraft in the airspace, we divide them into two groups, A and B. For each aircraft, if noncooperative obstacles appear within their detection range, we classify them as group A, otherwise we classify them as group B. The aircraft in group A have a higher priority than the aircraft in group B.
   a) For aircraft in group A, we prioritize them by comparing the risk levels between aircraft. The closer the obstacles are to their own position, the higher the priority of the aircraft.
   b) If the two aircraft in group A are threatened to a similar extent, then those with weaker maneuverability have a higher priority.
   c) If the two aircraft have the same maneuverability, then we can judge the priority by comparing their flight plan status through rule 3).
2) For aircraft in group B, that do not have static obstacles in the detection range, we classify them into B_1 and B_2 groups according to whether there is a risk of collision with other cooperation aircraft in the detection range. The B_1 group has a higher priority than the B_2 group.
   a) For aircraft in group B_1, we prioritize them by comparing the risk levels between aircraft. The closer the other aircraft are to their own position, the higher the priority of the aircraft.
   b) If the two aircraft in group A are threatened to a similar extent, then those with weaker maneuverability have a higher priority.
   c) If the two aircraft have the same maneuverability, then we can judge the priority by comparing their flight plan status through rule 3).
3) For aircraft in group B_2, each aircraft divides the set of viewable aircraft into two subsets: those within 5 nmi of their destination and all others. Aircraft in the first set have a higher rank than those in the second set.
   a) Within each set, aircraft are ranked according to the current flight delay, with a higher delay bringing a higher rank.
   b) Aircraft in the same set with the same delay are ranked by their current time in flight (which can also be interpreted as the remaining fuel endurance), with longer flight times resulting in a higher ranking.
   c) Finally, if all the above conditions are the same at the end, the shorter the remaining flight time, the higher the priority.

During the game process, aircraft with higher priority are usually more inclined to consider their own interests. While, aircraft with lower priority rankings need to consider more about the interests of the group, even making some sacrifices.

For threats with high risk of conflict, such as static obstacles, these noncooperative threats only need to consider their own preferences, all aircraft in the low-altitude airspace need to be given priority to avoid from the perspective of security. So, we regard them as the game neighbors with the highest priority. For cooperative aircraft, although they could transfer information to avoid collision, there also has potential conflict risks.

We assume that the ranking mechanism results in a unique priority for each player and that rankings within the same game are consistent from the perspectives of all players.

Based on this mechanism, we propose a neighbor set of x_i as X_i. X_i is defined as a set of players with higher priority than x_i and within the conflict set of x_i. Individuals with lower priority resolve those neglected potential conflicts.

3) Game Strategy Setting: In our game model, each UAV choose a strategy at each time step according to the positions and preferences of other aircraft or deterrents with which they would conflict. We propose HC and velocity-change mixed strategies of the game model. For this paper, we assume that all aircraft fly at the same altitude and the same initial speed

of 400 mph. The initial heading is from the start point to the destination for all UAVs. At each step, the aircraft can choose to change their velocity or angle according to the environment. For HC strategy, the aircraft has five directional options, including flying straight, moderate angle changing $\pm 5°$, and sharp angle changing $\pm 10°$. On the other hand, for the velocity-change strategy, aircrafts have five directional options, including constant speed, moderate velocity changing $\pm 5\%$, and sharp velocity changing $\pm 10\%$. Moreover, we consider two types of flights: 1) large-scale UAVs and 2) small UAVs. The main difference between them is mobility, where the velocity-change range is the best embodiment. For large-scale UAVs, the available velocity range is [200, 800] mph; flexible small UAVs is [150, 600] mph. In our model, there is no time interval for changing speeds or angles.

III. Satisficing CR Algorithm

In classical game theory, each player wants to obtain more benefit without considering the gains or losses of other players or the whole system. However, when using this concept on the flight conflict problem, a UAV is only concerned with his flight intention, which will lead to the entire airspace. Satisficing game theory [34] employs a new utility structure and a new solution concept, both of which easily accommodate cooperative agent communities and are therefore well matched with CR. The remaining alternatives are deemed to be good enough or satisficing. Mostly, an agent is a cautious optimizer who, rather than insisting on a single best solution, retains an enlarged view containing all reasonably acceptable solutions. Before describing the application of this new theory to CR, we summarize the essential components of satisficing game theory.

A. Social Utility

By forming a social utility function determined by decision maker's preferred behavior, satisfying game theory overcomes the limitation of traditional utility definition without considering conflict and cooperative energy. For a cooperative society formed by autonomous agents, the most basic requirement to ensure social stability is as following: the agents should be required under no circumstances benefit the group by hurting their own interests. Thus, the reasonable condition of forming cooperative society is to maintain social consistency, which means the arbitrary sacrifice of interests is not allowed. As established in [44], social coherence can be assured if and only if the preferences of a multi agent system are expressed by the mathematical syntax based on multivariate probability theory. Preferences are represented using social utilities, each of which is a mass function $p_G : S \to [0, 1]$, where S represents the set of possible actions. Social utilities must satisfy the following properties.

1) Nonnegativity: $p_G(s) \geq 0 \ \forall \ s \in S$.
2) Normalization: $s \in S \ p_G(s) = 1$.

Because social utilities are probability mass functions, and they have the properties of conditioning, independence, and marginalization.

A unique feature of satisficing game theory is the concept of dual utilities. Each individual X_i has two personalities: 1) selecting self S_i and 2) rejecting self R_i. Each S_i is associated with a selectable utility P_{S_i}, which orders each action available to X_i in terms of the effectiveness of the objective scheme without considering the cost or other consequences. Conversely, the rejectable utility P_{R_i} associated with each R_i orders each action in terms of the cost or other consequences. The individually satisficing set is defined as

$$\Sigma_i = \left\{ si \in S_i : p_{s_i}(s_i) \geq q_i p_{R_i}(s_i) \right\} \tag{4}$$

where S_i is the action set of X_i and q_i is a negotiation index.

Our satisficing CR algorithm is based on this dual utilities conception. A collision game is a multilayer structure, in which each player possesses a set of optional strategies and a mapping from different strategy combinations to the players' payoff. In response to this problem, we divide the calculation of the game revenue into two aspects. On the one hand, the security payoff (P_S) guarantees the flight safety of the entire airspace; on the other hand, the efficiency payoff (P_E) satisfies the requirements of individual aircraft to maximize their interests. The relationship of these two payoff is as follows.

1) We first consider the P_S, and get the security strategy set $\bar{S}_l$ as

$$\bar{S}_l = \left\{ s | s = \text{argmax}_{s_i^n \in S_i} P_S\left(s_i^n\right) \right\}, \bar{S}_l \subset S_i. \tag{5}$$

2) If there is more than one elememt in $\bar{S}_l$, we use P_E to select one satisfying strategy as

$$S_{\text{next}} = \text{argmax}_{s_i^n \in \bar{S}_l} P_E\left(s_i^n\right) \tag{6}$$

where S_{next} is the satisfying strategy of next step.

In the following, we described the security payoff (P_S) and the efficiency payoff (P_E) in detail.

B. Security Payoff

We first consider the requirements on flight safety. According to the number of conflicts and their degree of urgency, each strategy combination may cause its degree of urgency to obtain the first-level mapping of the elements within the strategy composition space. We represent the collision detection of the aircraft and the aircraft as the mapping of the Cartesian product space to the conflict space of the two-person strategy: $H : S_i \times S_j \to W^2$.

We define the strategy set $(s_1, s_2, \ldots, s_{M-1}, s_i)$ of aircraft $(x_1, x_2, \ldots, x_{M-1}, x_i)$, and we use v_i and Ang_i to represent the strategies that the aircraft can choose when they are involved in a conflict situation. For simplicity (but without loss of generality), we assume that the ranking orderings are $x_1, x_2, \ldots, x_{M-1}, x_i$, and x_i is with the lowest ranking. Let $v_c^1, v_c^2, \ldots, v_c^{M-1}, v_c^i$ and $(\text{Ang}_c^1, \text{Ang}_c^2, \ldots, \text{Ang}_c^{M-1}, \text{Ang}_c^i)$ signify the current speed and direction of $(x_1, x_2, \ldots, x_{M-1}, x_i)$; we thus have

$$P_S\left(s_i^n\right) = \frac{1}{1 + \sum_{j=1}^{M-1} F_S\left(s_i, s_j\right)}. \tag{7}$$

The function F_S is defined as

$$F_S\left(s_i^n, s_j\right) = \begin{cases} 2\beta, & d_{\min}(i,j) \le R_c \\ \beta, & R_c \le d_{\min}(i,j) \le R_{\text{nm}} \\ 0, & \text{otherwise} \end{cases} \tag{8}$$

where β is defined by

$$\beta = \begin{cases} \left(2 - \dfrac{d_{\min}(i,j)}{R_{\text{nm}}}\right)\left(\dfrac{1}{d_{k\min}(i,j)}\right)^{\alpha}, & d_{k\min}(i,j) \le 3R_{\text{nm}} \\ \left(\dfrac{1}{d_{k\min}(i,j)}\right)^{\alpha}, & \text{otherwise.} \end{cases} \tag{9}$$

The parameter α is an experimentally tuned variable, between 0 and 1. $d_{\min}(i,j)$ and $d_{k\min}(i,j)$ can be obtained by the conflict prediction function H. Those strategies with the maximum P_{CF} are seen as safety or subsafety [if v_i or Ang_i satisfy $P_S(s_i) = 1$] strategy sets $\bar{S}_l$

$$\bar{S}_l = \left\{ s | s = \text{argmax}_{s_i^n \in S_i} P_S\left(s_i^n\right) \right\}, \bar{S}_l \subset S_i. \tag{10}$$

C. Efficiency Payoff

When there is more than one element in $\bar{S}_l$, we need to choose one satisficing strategy from them. There are many constraints for UAVs in the CR problem; reaching the destination as quickly as possible is required in most flight missions. Hence, we define the RTA, which is another influencing factor when choosing a strategy. We assume that the $x_i's$ strategy set is $\bar{S}_l(\bar{v}_i, \overline{\text{Ang}_i})$, T_i^p represents the flight plan time of x_i, t_i^c is the current time that x_i has already flown, and t_i^d denotes the time of x_i selecting a strategy from $\bar{S}_l$ arriving at the destination. Then, the efficiency payoffs are defined by

$$P_E\left(\bar{S}_l\right) = \exp\left(-|t_i^c + t_i^d - T_i^p|\right) \tag{11}$$

where t_i^d is defined by

$$t_i^d = \frac{\overrightarrow{D_l^c D_l^d}}{\bar{v}_i} \tag{12}$$

$\overrightarrow{D_l^c}$ and $\overrightarrow{D_l^d}$ represent the current location and the destination location of x_i, and $\overrightarrow{D_l^c D_l^d}$ denotes the distance between these two places. The strategy with the maximum RTA payoffs will be executed by x_i in the next time step

$$S_{\text{next}} = \text{argmax}_{s_i^n \in S_i} P_E\left(s_i^n\right). \tag{13}$$

Finally, we obtain a satisfactory strategy and resolve the conflict.

IV. Evaluation and Results

In actual air traffic operations, the scenes of aircraft collisions are diverse. Thus, it is necessary to verify the effectiveness of the CR algorithm in different flight scenarios. Our simulation scenarios are divided into accessibility scenes and obstacle scenes, which are similar to those used in other studies [21], [45], [46]. Herein, accessibility scenes include perpendicular flows, choke point and random aircraft scenes; obstacle scenes include static obstacles in the above three scenarios. Although it is virtually impossible for these simulation scenarios to occur in actual flight, they are necessary to evaluate the extreme performance of the CR algorithm, and it is also convenient to compare with different methods.

In the above scenarios, we adopt three flight strategy adjustment models, HC, velocity-HC (VHC), and heterogeneous-VHC (HVHC), herein aiming to study the effects of angle adjustment, speed changing, and their combination on the CR. For HC strategies, there are only five directional options: flying straight, moderate angle changing $\pm 5°$, and sharp angle changing $\pm 10°$. For velocity-change strategy, aircrafts have five directional options, including constant speed, moderate velocity changing $\pm 5\%$, and sharp velocity changing $\pm 10\%$. Moreover, we consider two types of flights speed limitation range: A larger one is [200, 800] mph, and a smaller scale is [150, 600] mph. HC model only adopts five HC strategies. VHC model is consist of HC strategy and velocity-change strategies for large speed range. HVHC model is composed of HC strategy, velocity-change strategies for both two speed changing ranges.

Our structure map is a 100×100 square lattices, where the lattice resolution is 1:1 nmi. The detection margin is $R_d = 10$ nmi, the near-miss margin is $R_{\text{NM}} = 1$ nmi, and the collision margin is $R_c = 500$ ft.

The parameter setting for the accessibility scenes is as follows. The standard deviation $\sigma_x = \sigma_y = 4.0$. The predicted time $T_w = 2$ min.

The obstacle scenes have the following parameter setting: The standard deviation $\sigma_x = \sigma_y = 5.0$. The predicted time $T_w = 4$ min. The forbidden zone margin for obstacles is $R_F = 100$ ft.

A. Performance Measures

To evaluate our performance of the approaches, we must use appropriate metrics to ensure that both safety and performance objectives are met. Safety and system efficiency evaluation concerns are similar to those in [34]. System efficiency is a vital evaluation index for ensuring that the aircraft can follow directions, linear flight paths to their destinations. CR maneuvers should meet safety criteria while providing high levels of efficiency.

1) System Efficiency: We define the individual efficiency for aircraft i as $E_i = [t_i^p/(t_{d_i} + t_i^p)]$, where t_i^p is the ideal flight time of the aircraft in plan and t_{d_i} is the added delay time. Then, the system efficiency is given by

$$E = \frac{1}{N}\sum_{i=1}^{N} E_i \tag{14}$$

where N is the number of aircraft in the system. $E = 1$ is an ideal scheme, and as the traffic density and congestion increase or there are deterrents in the airspace, the aircraft's flight conditions further deviate from their plan, and E decreases in value.

2) Risk Factor: For each CR algorithm, the most important evaluation index is the safety capability. In complex low-altitude airspace, the frequency of conflict is related to the complexity level of the airspace and the density of UAVs. In this paper, we propose two indicators to evaluate the safety of

our method. One indicator is the near miss coefficient (F_{NM}), which expresses the average occurrence ratio of near-miss incidents in a time unit; F_{NM} is defined as

$$F_{\mathrm{NM}} = \frac{\sum_{i=1}^{T_{\mathrm{all}}} F_{\mathrm{NM}}^{i}}{T_{\mathrm{all}}}. \tag{15}$$

F_{NM}^{t} represents the number of near-miss incidents occurred in the ith time step. T_{all} is the total time of the conflict game process. Another indicator is the system collision number, which is defined by

$$F_{C} = \frac{\sum_{i=1}^{T_{\mathrm{all}}} F_{C}^{i}}{T_{\mathrm{all}}}. \tag{16}$$

F_C represents the number of collision incidents occurring in the ith time step.

In complex low-altitude environments, potential aircraft collision events exhibit diverse characteristics, so we need to verify the effectiveness of the aircraft hedging method in different flight scenarios. Combined with the particularity of the complex low-altitude environment, this paper establishes 2-D scenes from three aspects based on the experimental scenarios provided in [47]. The first is whether there are noncooperative threats in the flight scene. This part of the experiment verifies the security and effectiveness of the proposed method from two aspects: 1) accessibility scenes without obstacles and 2) complex scenes with obstacles. Then, considering the influence of airspace density on the CR method, we partially verifies the safety and effectiveness of the proposed method in different aircraft density scenarios. It is important to notice that some scenes with high aircraft density are almost impossible to happen in reality, these extreme scenarios help in the study of the capabilities and limitations of any CR design. Finally, the experimental part verifies the adaptability of the algorithm in the flight scenario with strong randomness from the perspective of method robustness.

In this part of the experiment, we also analyze the impact of different CR strategies on the risk aversion effect. In terms of CR strategies, we propose three different strategies: 1) HC strategy; 2) VHC strategy; and 3) HVHC strategy.

Finally, this experiment extends the algorithm to 3-D space, and verifies the applicability and security of the proposed method in 3-D space.

B. 2-D Scenes

To identify our approach, we propose flow scenes, choke point scenes, and random flight scenes as evaluation cases, where each scenes also has two aspects: 1) accessibility scene and 2) obstacle scene. In the following experiments, we adopt accessibility scenes at first. Then, introducing static obstacles into the accessibility scenes to further examine our algorithm.

1) Flow Scenes: First, we adopt the scenes introduced in [47]. In these scenes, two direct traffic constant flows perpendicular to the direction of flight within an $L \times L$ ($L = 100$ nmi) airspace, as depicted in Fig. 3(a). In the perpendicular flow scene, one flow is moving from left to right, and the other flow is moving from bottom to top. This scenes have potential conflicts at the intersection point, and the aircraft can autonomously avoid hazards. Based on the perpendicular flow scene, we site an $r = 5$ nmi circular obstacle at the center of the scene, as depicted in Fig. 3(b).

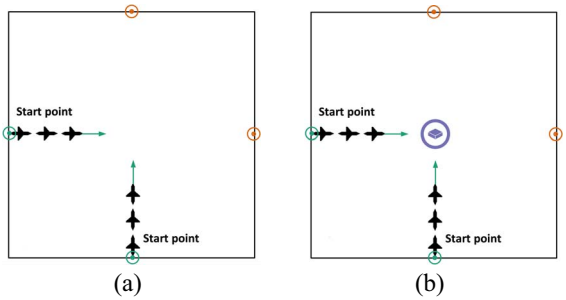

Fig. 3. Flow scenes. (a) Perpendicular flow accessibility scene. (b) Perpendicular flow obstacle scene.

The two cases of flow scenario are presented with 16 agents at different time step (T) as shown in Fig. 4. The starting point is marked in green and the destination point is denoted with orange. Fig. 4(a), (c), and (e) is the result for perpendicular flow scenario and Fig. 4(b), (d), and (f) is for perpendicular flow scenario with obstacle. The simulation result shows the process of CR. It shows that the satisficing CR algorithm performs well when solving the collision.

In a given flow, all aircraft are generated at the same point with the same destination, and the interval between two neighboring aircraft is τ seconds. τ is a traffic density control parameter, where a smaller τ means denser traffic. Note that τ should be large enough to create a separation from the anterior aircraft to avoid violating its safety margin with the aircraft immediately behind it. In our method, aircraft are generated 20 s apart, keeping an approximately 2 nmi distance from the previous aircraft. Therefore, each aircraft can maintain a safety margin with the other aircraft, which are generated from the same flow.

To analyze the influence of τ on the security of the UAVs, we choose HVHC model under the opposite flow scene with density $=$ 16. The results are averaged over 20 independent experiments.

After the experimental statistics are obtained, with increasing τ, we find that the collision number is always 0 under the HC, VHC, and HVHC strategies. However, the main difference between the three strategies is the average number of near misses and the system efficiency. Fig. 5 reports the average number of near misses under the HC, VHC, and HVHC strategies in the perpendicular flow scenario. With increasing τ, the probability of a near miss occurring decreases, which shows that the security of the UAVs has been improved and that the system is more efficient. Moreover, for the VHC and HVHC strategies, when τ is large, the effect of τ on the system efficiency is significant. Then, we also examine the system efficiency and near misses for HVHC model with τ under the perpendicular flow scenario with obstacle, as shown in Fig. 6. The different value of the system efficiency shows that only changing the heading leads to a flight delay because this strategy choice increases the flight path length, and the UAV could not catch up to the flight schedule. Nevertheless, the mixed

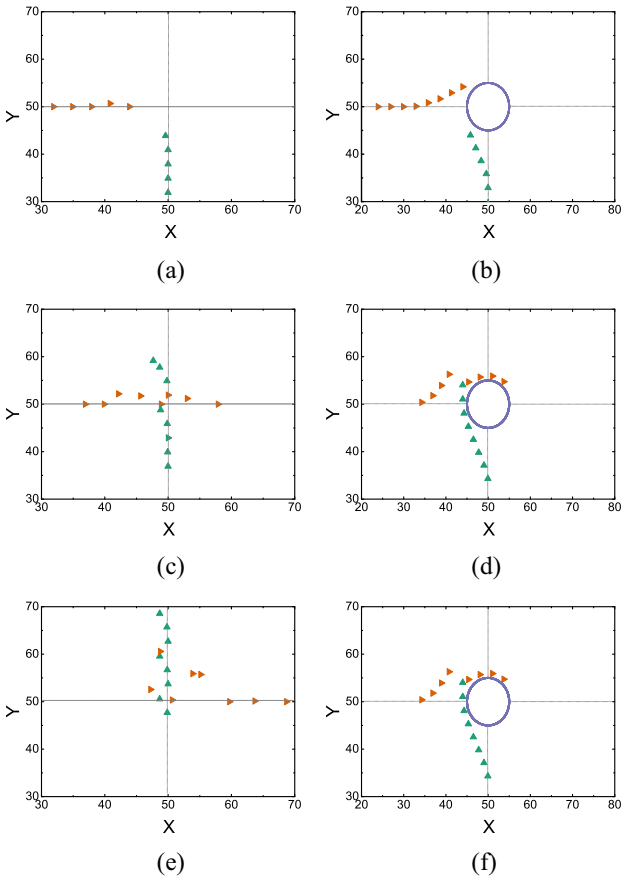

Fig. 4. Simulation result for flows scenes. (a) Perpendicular flow accessibility scene at $T = 450$. (b) Perpendicular flow obstacle scene at $T = 400$. (c) Perpendicular flow accessibility scene at $T = 550$. (d) Perpendicular flow obstacle scene at $T = 550$. (e) Perpendicular flow accessibility scene at $T = 650$. (f) Perpendicular flow obstacle scene at $T = 750$.

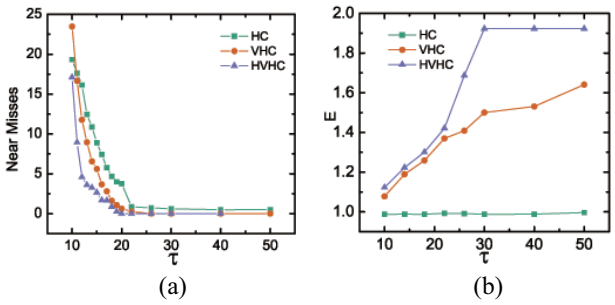

Fig. 5. Result for perpendicular flow senario over HVHC model. (a) Near misses with τ. (b) System efficiency with τ.

strategies of changing both the heading and the velocity could help the UAV in changing its flight plan when this UAV overcomes the obstacle in this scene. Moreover, the heterogeneous velocity changing strategy varies the UAVs' mobility, thereby achieving an optimal system efficiency.

2) Choke Point Scenes: In the choke point accessibility scene, all aircraft begin from uniformly spaced points on a circle of radius L ($L = 100$ nmi), with the point on the circle directly opposite each aircraft's starting point as its destination. Fig. 7(a) shows an example of eight UAVs, where the planned paths coincide at the center of the circle. Although

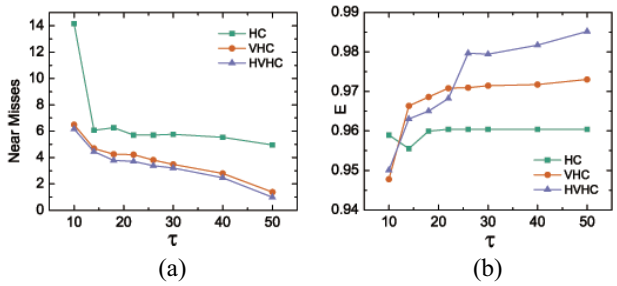

Fig. 6. Result for perpendicular flow senario with obstacle over HVHC model. (a) Near misses with τ. (b) System efficiency with τ.

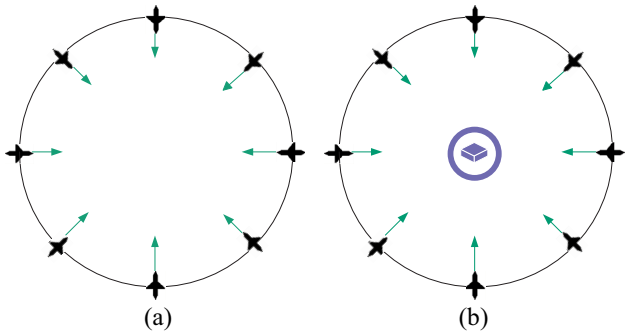

Fig. 7. Choke point scenes. (a) Choke point accessibility scene. (b) Choke point obstacle scene.

this scenario is not representative of actual traffic patterns, it is a significant challenge for any CR algorithm. In the choke point obstacle scene, we set an $r = 5$ nmi circle obstacle at the center of this scenario to make the airspace more complicated, as shown in Fig. 7(b).

Fig. 8(a), (c), and (e) presents the simulation results of a run with 4, 8, and 16 aircraft under HVHC model in the choke point accessibility scene. Fig. 8(b), (d), and (f) presents the simulation result of a run with 4, 8, and 16 aircrafts under the three models. The aircraft could avoid both meeting and the obstacle simultaneously at the center and reach their destinations at the planned time through speed and angle adjustments. The existence of the obstacle could decentralized the conflict from the center of the scene to some extent.

Table I summarizes the variation trend of the three performance measures during the simulation phase with increasing density of aircraft. It shows that the UAVs can resolve conflicts completely; however, as the density of aircraft increases, the conflict risk and system time delay increase significantly. For HC model, although there are risks during the process of CR, the conflict events can typically be resolved. However, comparing with VHC and HVHC model, the system efficiency over HC model is obviously decreased. Heading changes cause the aircraft to deviate from the planned flight path, but the aircraft still keeps the planned speed. Consequently, the actual flight time of the aircraft will increase, resulting in reduced system efficiency. For VHC model the aircraft can eliminate or reduce the flight delay caused by deviations from the planned flight path through angular deflection and appropriate acceleration flight. Moreover, the conflict risk and system efficiency are better

TABLE I
RESULTS FOR THE CHOKE POINT ACCESSIBILITY SCENES

	HC			VHC			HVHC		
Density	E (%)	NM	C	E(%)	NM	C	E(%)	NM	C
4	1.0000	0.744463	0	0.992652	0.492582	0	1.009591	0.47960	0
8	0.994857	3.500181	0	0.998846	0.605553	0	1.009464	0.487258	0
12	0.978021	5.947344	0	1.00424	4.403130	0	1.009337	2.646538	0
16	0.977503	3.573473	0	1.008400	2.895105	0	1.009087	2.464184	0
20	0.931650	8.740841	0.052490	1.006785	7.759781	0	1.009185	5.774666	0
24	0.947372	12.117716	0	1.009043	8.233814	0	1.009004	7.415136	0
28	0.952821	9.387480	0	1.009085	11.854613	0.055894	1.009084	10.086952	0
32	0.930219	14.790979	0.080030	1.008910	12.843921	0.025568	1.007997	10.513973	0

TABLE II
RESULT FOR THE CHOKE POINT OBSTACLE SCENES

	HC			VHC			HVHC		
Density	E (%)	NM	C	E(%)	NM	C	E(%)	NM	C
4	0.978474	12.497554	0	1.001037	6.765935	0	1.008574	6.694268	0
8	0.978474	11.777642	0	0.998031	6.668539	0	1.007198	6.581548	0
12	0.978474	12.497554	0	1.001661	7.029977	0	1.008081	6.979977	0
16	0.978833	12.380496	0	1.001068	8.975779	0	1.004213	7.431526	0
20	0.978905	13.049718	0	1.001393	6.441785	0	1.005892	6.161882	0
24	0.978833	12.712826	0	1.003611	7.450392	0	1.002797	7.124814	0
28	0.978610	12.490516	0	0.999610	5.320271	0	1.003881	5.252466	0
32	0.978863	13.350197	0	1.003955	6.374149	0	1.002837	6.337001	0

TABLE III
RESULTS FOR THE RANDOM FLIGHT ACCESSIBILITY SCENE

	HC			VHC			HVHC		
Density	E (%)	NM	C	E(%)	NM	C	E(%)	NM	C
4	1.0000	0	0	1.018168	0	0	1.022707	0	0
8	0.992222	1.972304	0	1.014823	0.496791	0	1.020667	0.201316	0
12	0.995152	3.311164	0	1.013294	1.325044	0	1.015778	0.526675	0
16	0.983033	5.668644	0	1.008950	4.009714	0	1.010692	3.099443	0
20	0.973083	11.607371	0.100000	1.004819	6.376046	0.299552	1.006808	5.421804	0.037365
24	0.968069	13.543463	0.249559	0.983538	8.201220	0.108863	0.994176	7.700879	0.026483
28	0.954430	14.735785	0.286295	0.976713	13.763946	0.236549	0.986328	9.278112	0.027829
32	0.953620	15.28052	0.301670	0.971352	14.028424	0.270174	0.978432	12.409149	0.164320

than under HVHC model because the flexibility of multiple aircraft has been best considered.

With increased flight density, the airspace becomes crowded, and the security of the UAVs becomes difficult to guarantee. Table II summarizes the variation trend of the three performance measures under the choke point scene with the obstacle. The table shows that the UAVs can resolve conflicts completely; however, as the density of the aircraft increased, the conflict risk and system time delay increased significantly. Compared with the accessibility scene, the near miss risk increases but there is no collision risk, and the efficiency decreases. Although the obstacle occupy the active range of UAVs, it decentralized the conflict point.

3) Random Flights Scenes: This scenario consists of two concentric circles as used in [48]. The aircraft starting points are on the outer circle (radius of 50 nmi), and the destination points are randomly selected on the inner circle (radius of 40 nmi), as described in Fig. 9. The 10-nmi buffer between the circles is to avoid the appearance of conflict initially. Due to the random geometric structure of this scene, this is a useful method of verifying the effectiveness of the CR algorithm.

At the beginning of each simulation, a new aircraft is generated every 5 s on the outer circle at a random position until the number of aircraft in the scene reaches the specified upper limit. We use the relevant traffic density parameter N to represent the top limitation of the number of aircraft in the scene. When the aircraft arrives at the destination, a new aircraft will be created to replace it. These new aircraft have the same starting and ending points as the aircraft that have just arrived at the destination. In the simulation, the results obtained were averaged after 20 separate runs. The result for aircraft density of $N = 6$ over HVHC model is shown in Fig. 10(a) for a single running under random flights accessibility scene,

TABLE IV
RESULTS FOR THE RANDOM FLIGHTS OBSTACLE SCENES

	HC			VHC			HVHC		
Density	E (%)	NM	C	E(%)	NM	C	E(%)	NM	C
4	0.998585	2.523428	0	1.020352	1.659574	0	1.022728	0.306220	0
8	0.998034	5.362933	0	1.011087	3.103819	0	1.020715	1.454765	0
12	0.996804	7.616322	0	1.006405	5.430613	0	1.018586	3.404074	0
16	0.986289	11.754264	0	1.003180	8.795146	0	1.008518	4.627102	0
20	0.983078	12.836107	0.105469	0.993720	10.041820	0.027760	1.002926	6.437842	0.01380
24	0.977555	14.685294	0.212110	0.989936	12.003131	0.070878	0.997156	10.295053	0.071136
28	0.965287	17.274623	0.331366	0.982403	13.847128	0.287962	0.986789	13.578415	0.233249
32	0.951584	18.059578	0.428746	0.970382	15.798623	0.384751	0.978324	14.289763	0.274631

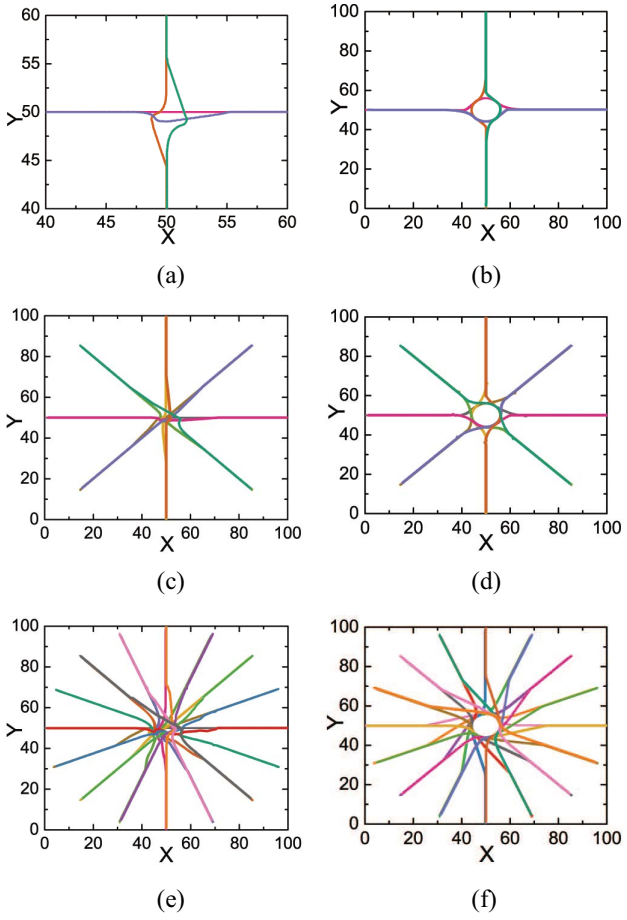

Fig. 8. Simulation result for choke point scenes. (a) Choke point accessibility scene for 4 UAVs. (b) Choke point obstacle scene for 4 UAVs. (c) Choke point accessibility scene for 8 UAVs. (d) Choke point obstacle scene for 8 UAVs. (e) Choke point accessibility scene for 16 UAVs. (f) Choke point obstacle scene for 16 UAVs.

and $N = 5$ for random flights obstacle scene as shown in Fig. 10(b).

Tables III and IV summarize the average number of collisions and near misses and the system efficiency E as the aircraft density increases for random flight accessibility and obstacle scene, respectively. The results suggest that situations occasionally arise in the random flight scenario that is difficult to resolve. The frequency of separation violations increases as the traffic density increases, and considering

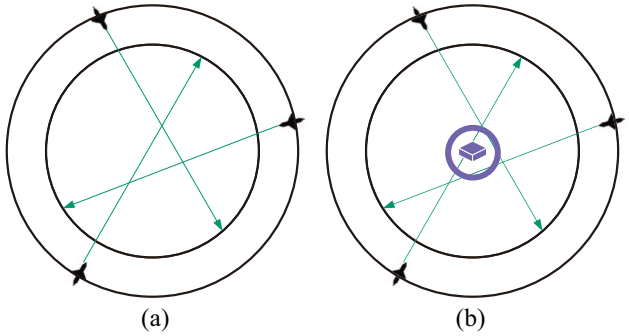

Fig. 9. Random flights scene. (a) Random flights accessibility scene. (b) Random flights obstacle scene.

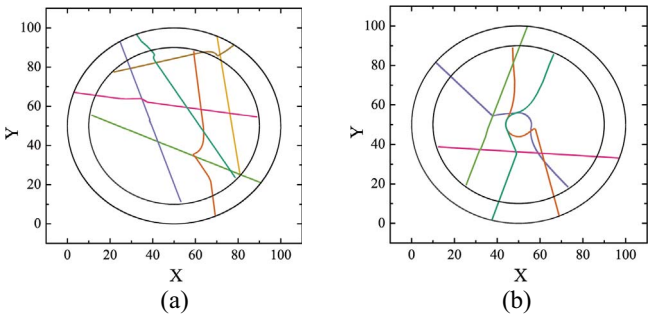

Fig. 10. Simulation result for random flights scenes. (a) Random flights accessibility scene. (b) Random flights obstacle scene.

the strategies with velocity changes can improve the system efficiency.

In the following experiments, we evaluate the performance of the CR method using 3-D scenes.

C. 3-D Scene

In this section, we examine the CR algorithm in 3-D random flight scene. Based on the original game strategy setting rules of 2-D scenes, we introduce pitch-angle-change strategy, including flying straight, moderate pitch angle changing $\pm 2.5°$, sharp angle changing $\pm 5°$. Thus, we extend HVHC strategy to velocity-heading-pitch-angle-change model (HVHPC). The 3-D scene is a $L \times L \times L$ ($L = 100$ nmi) airspace, as shown in Fig. 11, the start points of aircraft are randomly generated on the bottom plane and the destination point are randomly generated on the top plane. There are nine

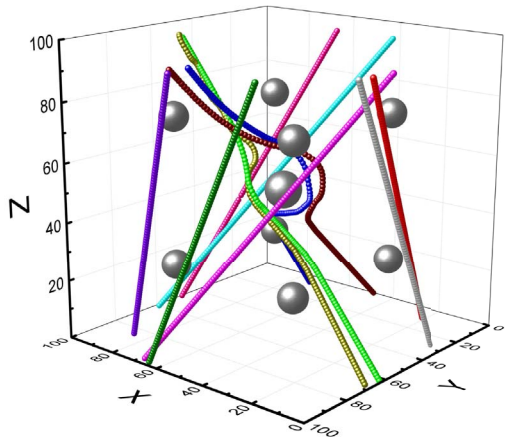

Fig. 11. Simulation result for 3-D random flights scene with obstacle.

TABLE V
RESULTS FOR THE 3-D RANDOM FLIGHTS OBSTACLE SCENE

HVHPC			
Density	E (%)	NM	C
4	0.537684	0.496324	0
8	0.450159	0.614981	0
12	0.403584	0.423032	0
16	0.569194	0.695913	0
20	0.473211	0.959518	0
24	0.477867	1.605846	0
28	0.442736	3.432924	0
32	0.592349	4.793429	0.086730

obstacles (gray balls) in the 3-D scene, one is at the center point (50, 50, 50) and its radius is 10 nmi, the other eight static obstacles' coordinates are (25, 25, 25), (25, 25, 75), (25, 75, 25), (25, 75, 75), (75, 25, 25), (75, 25, 75), (75, 75, 25), and (75, 75, 75) and their radius are 5 nmi. The result for aircraft density of $N = 12$ over HVHPC strategy is shown in Fig. 11 for a single run. Table V summarizes the variation trend of the three performance measures over HVHPC strategy with the increment of aircraft density (N). Moreover, we extend the uncertainty Gaussian model to a trivariate one in 3-D scenes. The simulation results shown that, with the increasing of N, the collision only occurred for the maximum density, the near miss risk is increasing, the system efficiency changes of a fluctuating. To summarize, our algorithm can satisfying solve the conflict problems in 3-D scene.

V. CONCLUSION

We investigated the CR problem of multiple UAVs and proposed a satisficing CR algorithm based on satisficing game theory. By applying three models, HC, VHC, and heterogenous-VHC, we built two simulation scenarios, accessibility scenes, and obstacle scenes, to validate the proposed algorithm and study the different influences of velocity and heading on the CR. Furthermore, we proposed a 3-D random flights obstacle scene to further examine our algorithm. Nevertheless, in the proposed algorithm, we only use a circle to define the safety area of the obstacles. In the future, we need to analyze the heterogeneity of multiple obstacles and design a more appropriate safety envelope that can adjust its shape depending on different characteristics of the obstacles.

ACKNOWLEDGMENT

The authors would like to thank X. Cao, G. Xiao, and H. Li for useful discussions.

REFERENCES

[1] M. DeGarmo and G. Nelson, "Prospective unmanned aerial vehicle operations in the future national airspace system," in *Proc. AIAA 4th Aviation Technol. Integr. Oper. (ATIO) Forum*, 2004, p. 6243.
[2] M. Nolan, *Fundamentals of Air Traffic Control*, 4th ed. Belmont, CA, USA: BrooksICole-Thomson Learn., 2004.
[3] National Research Council, *The Future of Air Traffic Control: Human Operators and Automation*. Washington, DC, USA: Nat. Acad. Press, 1998.
[4] R. Schultz *et al.*, "Free flight concept," in *Proc. Guid. Navig. Control Conf.*, 1997, p. 3677.
[5] F. Yang, J. Li, T. Lei, and S. Wang, "Architecture and key technologies for Internet of Vehicles: A survey," *J. Commun. Inf. Netw.*, vol. 2, no. 2, pp. 1–17, 2017.
[6] L. Sun, A. Huang, H. Shan, and L. Cai, "Adaptive beaconing for collision avoidance and tracking accuracy in vehicular networks," *J. Commun. Inf. Netw.*, vol. 2, no. 2, pp. 30–45, 2017.
[7] C. Lin, Y. Bi, H. Zhao, Z. Wang, and J. Wang, "Scheduling algorithms for time-constrained big-file transfers in the Internet of Vehicles," *J. Commun. Inf. Netw.*, vol. 2, no. 2, pp. 126–135, 2017.
[8] M. Mozaffari, W. Saad, M. Bennis, and M. Debbah, "Unmanned aerial vehicle with underlaid device-to-device communications: Performance and tradeoffs," *IEEE Trans. Wireless Commun.*, vol. 15, no. 6, pp. 3949–3963, Jun. 2016.
[9] Y. Zeng, R. Zhang, and T. J. Lim, "Wireless communications with unmanned aerial vehicles: Opportunities and challenges," *IEEE Commun. Mag.*, vol. 54, no. 5, pp. 36–42, May 2016.
[10] *Aerospace Forecasts 2016–2036*, FAA, Washington, DC, USA, 2016. [Online]. Available: http://www.faa.gov/data research/aviation/
[11] K. Dalamagkidis, K. P. Valavanis, and L. A. Piegl, *On Integrating Unmanned Aircraft Systems Into the National Airspace System: Issues, Challenges, Operational Restrictions, Certification, and Recommendations*, vol. 54. Dordrecht, The Netherlands: Springer, 2011.
[12] J. Tang, S. Alam, C. Lokan, and H. A. Abbass, "A multi-objective approach for dynamic airspace sectorization using agent based and geometric models," *Transport. Res. C Emerg. Technol.*, vol. 21, no. 1, pp. 89–121, 2012.
[13] A. Chakravarthy and D. Ghose, "Obstacle avoidance in a dynamic environment: A collision cone approach," *IEEE Trans. Syst., Man, Cybern. A, Syst., Humans*, vol. 28, no. 5, pp. 562–574, 1998.
[14] K. D. Bilimoria, "A geometric optimization approach to aircraft conflict resolution," in *Proc. AIAA Guid. Navig. Control Conf. Exhibit*, vol. 6, 2000, pp. 14–17.
[15] Z.-H. Mao, D. Dugail, E. Feron, and K. Bilimoria, "Stability of intersecting aircraft flows using heading-change maneuvers for conflict avoidance," *IEEE Trans. Intell. Transp. Syst.*, vol. 6, no. 4, pp. 357–369, Dec. 2005.
[16] J. Tang, L. Fan, and S. Lao, "Collision avoidance for multi-UAV based on geometric optimization model in 3D airspace," *Arabian J. Sci. Eng.*, vol. 39, no. 11, pp. 8409–8416, 2014.
[17] O. Khatib, "Real-time obstacle avoidance for manipulators and mobile robots," *Int. J. Robot. Res.*, vol. 5, no. 1, pp. 90–98, 1986.
[18] M. S. Eby, "A self-organizational approach for resolving air traffic conflicts," *Lincoln Lab. J.*, vol. 7, no. 2, pp. 239–254, 1994.
[19] L. Xiang, X. Qinghua, and D. Tao, "An artificial potential field model with constraints," in *Proc. IEEE 31st Chin. Control Conf. (CCC)*, 2012, pp. 4680–4683.
[20] K. Zeghal, "A comparison of different approaches based on force fields for coordination among multiple mobiles," in *Proc. IEEE/RSJ Int. Conf. Intell. Robots Syst.*, vol. 7, 1998, pp. 273–278.

[21] K. Zeghal, "A review of different approaches based on force fields for airborne conflict resolution," in *Proc. AIAA Guid. Navig. Control Conf.*, vol. 7, 1998, pp. 818–827.
[22] A. G. Sanfey, J. K. Rilling, J. A. Aronson, L. E. Nystrom, and J. D. Cohen, "The neural basis of economic decision-making in the ultimatum game," *Science*, vol. 300, no. 5626, pp. 1755–1758, 2003.
[23] X. Kang, R. Zhang, and M. Motani, "Price-based resource allocation for spectrum-sharing femtocell networks: A Stackelberg game approach," *IEEE J. Sel. Areas Commun.*, vol. 30, no. 3, pp. 538–549, Apr. 2012.
[24] H.-Y. Shi, W.-L. Wang, N.-M. Kwok, and S.-Y. Chen, "Game theory for wireless sensor networks: A survey," *Sensors*, vol. 12, no. 7, pp. 9055–9097, 2012.
[25] C. Jiang, Y. Chen, Y. Gao, and K. J. R. Liu, "Joint spectrum sensing and access evolutionary game in cognitive radio networks," *IEEE Trans. Wireless Commun.*, vol. 12, no. 5, pp. 2470–2483, May 2013.
[26] C. Jiang *et al.*, "Machine learning paradigms for next-generation wireless networks," *IEEE Wireless Commun.*, vol. 24, no. 2, pp. 98–105, Apr. 2017.
[27] K. Ganeshpure and S. Kundu, "Game theoretic approach for run-time task scheduling on an multi-processor system on chip," *IET Circuits Devices Syst.*, vol. 7, no. 5, pp. 243–252, 2013.
[28] G. J. Pappas, C. Tomlin, and S. Sastry, "Conflict resolution for multi-agent hybrid systems," in *Proc. 35th IEEE Conf. Decis. Control*, vol. 2, 1996, pp. 1184–1189.
[29] C. Tomlin, G. J. Pappas, and S. Sastry, "Noncooperative conflict resolution [air traffic management]," in *Proc. 36th IEEE Conf. Decis. Control*, vol. 2, 1997, pp. 1816–1821.
[30] R. Lachner, "Collision avoidance as a differential game: Real-time approximation of optimal strategies using higher derivatives of the value function," in *Proc. IEEE Int. Conf. Syst. Man Cybern. Comput. Cybern. Simulat.*, vol. 3, 1997, pp. 2308–2313.
[31] J. Zhang and S. Sastry, "Aircraft conflict resolution: Lie–Poisson reduction for game on SE(2)," in *Proc. 40th IEEE Conf. Decis. Control*, vol. 2, 2001, pp. 1663–1668.
[32] A. Bayen, S. Santhanam, I. Mitchell, and C. Tomlin, "A differential game formulation of alert levels in ETMS data for high altitude traffic," in *Proc. AIAA Guid. Navig. Control Conf. Exhibit*, 2003, p. 5341.
[33] C. Tomlin, I. Mitchell, and R. Ghosh, "Safety verification of conflict resolution manoeuvres," *IEEE Trans. Intell. Transp. Syst.*, vol. 2, no. 2, pp. 110–120, Jun. 2001.
[34] J. K. Archibald, J. C. Hill, N. A. Jepsen, W. C. Stirling, and R. L. Frost, "A satisficing approach to aircraft conflict resolution," *IEEE Trans. Syst., Man, Cybern. C, Appl. Rev.*, vol. 38, no. 4, pp. 510–521, Jul. 2008.
[35] L. Bai, L. Zhu, X. Zhang, W. Zhang, and Q. Yu, "Multi-satellite relay transmission in 5G: Concepts, techniques, and challenges," *IEEE Netw.*, vol. 32, no. 5, pp. 38–44, Sep./Oct. 2018.
[36] Q. Yu, C. Han, L. Bai, J. Choi, and X. S. Shen, "Low-complexity multiuser detection in millimeter-wave systems based on opportunistic hybrid beamforming," *IEEE Trans. Veh. Technol.*, vol. 67, no. 10, pp. 10129–10133, Oct. 2018.
[37] Q. Yu, J. Wang, and L. Bai, "Architecture and critical technologies of space information networks," *J. Commun. Inf. Netw.*, vol. 1, no. 3, pp. 1–9, 2016.
[38] S. Arumugam and C. Jermaine, "Closest-point-of-approach join for moving object histories," in *Proc. IEEE 22nd Int. Conf. Data Eng. (ICDE)*, 2006, pp. 86–86.
[39] S. Thrun, *Probabilistic Robotics*. Cambridge, MA, USA: MIT Press, 2005.
[40] D. Rathbun, S. Kragelund, A. Pongpunwattana, and B. Capozzi, "An evolution based path planning algorithm for autonomous motion of a UAV through uncertain environments," in *Proc. IEEE 21st Digit. Avionics Syst. Conf.*, vol. 2, 2002, pp. 1–12.
[41] M. Prandini, J. Hu, J. Lygeros, and S. Sastry, "A probabilistic approach to aircraft conflict detection," *IEEE Trans. Intell. Transp. Syst.*, vol. 1, no. 4, pp. 199–220, Dec. 2000.
[42] K. D. McDonald *et al.*, "The modernization of GPS: Plans, new capabilities and the future relationship to Galileo," *Positioning*, vol. 1, no. 3, pp. 1–17, 2002.
[43] K. Katsaros and M. Dianati, "A cost-effective SCTP extension for hybrid vehicular networks," *J. Commun. Inf. Netw.*, vol. 2, no. 2, pp. 18–29, 2017.
[44] W. C. Stirling, "Social utility functions—Part I: Theory," *IEEE Trans. Syst., Man, Cybern. C, Appl. Rev.*, vol. 35, no. 4, pp. 522–532, Nov. 2005.
[45] C. Luo, S. I. McClean, G. Parr, L. Teacy, and R. De Nardi, "UAV position estimation and collision avoidance using the extended Kalman filter," *IEEE Trans. Veh. Technol.*, vol. 62, no. 6, pp. 2749–2762, Jul. 2013.
[46] S. Ragi and E. K. P. Chong, "UAV path planning in a dynamic environment via partially observable Markov decision process," *IEEE Trans. Aerosp. Electron. Syst.*, vol. 49, no. 4, pp. 2397–2412, Oct. 2013.
[47] D. Dugail, E. Feron, and K. Bilimoria, "Stability of intersecting aircraft flows using heading change maneuvers for conflict avoidance," in *Proc. IEEE Amer. Control Conf.*, vol. 1, 2002, pp. 760–766.
[48] J. Krozel, M. Peters, K. D. Bilimoria, C. Lee, and J. S. Mitchell, "System performance characteristics of centralized and decentralized air traffic separation strategies," *Air Traffic Control Quart.*, vol. 9, no. 4, pp. 311–332, 2001.

Yumeng Li (S'17) received the B.S. degree from the College of Information and Communication Engineering, Harbin Engineering University, Harbin, China, in 2016. She is currently pursuing the Ph.D. degree in information and communication engineering at Beihang University, Beijing, China.

Her current research interests include network science, unmanned aerial vehicle conflict resolution, and swarm intelligence systems.

Wenbo Du (M'17) received the B.S. and Ph.D. degrees from the School of Computer Science and Technology, University of Science and Technology of China, Hefei, China, in 2005 and 2010, respectively.

He is an Associate Professor with the School of Electronic and Information Engineering, Beihang University, Beihang, China. His current research interests include network science and bio-inspired computation.

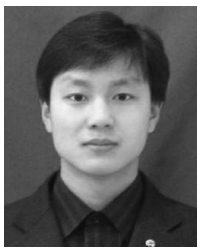

Peng Yang is currently pursuing the Ph.D. degree in information and communication engineering at Beihang University, Beijing, China.

His current research interests include intelligent transportation systems, Internet of Things and sensor network, next-generation mobile cellular systems, and unmanned aerial vehicle networks.

Tianhang Wu received the B.S. degree in communication engineering from the Honor School, Harbin Institute of Technology, Harbin, China, in 2011, and the Ph.D. degree in traffic information engineering and control with Beihang University, Beijing, China, in 2018.

Since 2018, he has been with the Beijing Institute of Radio Measurement, Beihang. His current research interests include computer vision, aircraft autonomy conflict avoidance, game theory, and machine learning.

Jun Zhang received the B.S., M.Sc., and Ph.D. degrees from Beihang University, Beijing, China, in 1987, 1991, and 2001, respectively.

He is currently a Member of the China Engineering Academy and the President with the Beijing Institute of Technology, Beijing. His current research interests include integrated networks of air, ground, and sky communication systems, modern air traffic management, ad hoc networks, and network management.

Dapeng Wu (S'98–M'04–SM'06–F'13) received the B.E. degree in electrical engineering from the Huazhong University of Science and Technology, Wuhan, China, in 1990, the M.E. degree in electrical engineering from the Beijing University of Posts and Telecommunications, Beijing, China, in 1997, and the Ph.D. degree in electrical and computer engineering from Carnegie Mellon University, Pittsburgh, PA, USA, in 2003.

He is currently a Professor with the Department of Electrical and Computer Engineering, University of Florida, Gainesville, FL, USA. His current research interests include networking, communications, signal processing, computer vision, machine learning, smart grid, and information and network security.

Matjaž Perc received the Ph.D. degree with his thesis on noise-induced pattern formation in spatially extended systems with applications to the nervous system, game-theoretical models, and social complexity.

In 2010, he became the Head of the Institute of Physics, University of Maribor, Maribor, Slovenia, where he became a Full Professor of physics in 2011. In 2015, he established the Complex Systems Center Maribor. He is currently a Professor of physics with the University of Maribor, where he is the Director of the Complex Systems Center Maribor. His current research interests include media and professional literature.

Dr. Perc was a recipient the Young Scientist Award for Socio-physics and Econo-physics in 2015, one of the most cited physicists according to Thomson Reuters, and the Zois Certificate of Recognition for Outstanding Research Achievements in Theoretical Physics in 2009. He is a member of Academia Europaea. He is an Outstanding Referee of the *Physical Review* and *Physical Review Letters* journals and a Distinguished Referee of *Europhysics Letters*.